Article

Not peer-reviewed version

# Upregulation of Transferrin Receptor 1 (TfR1) at the Blood-Brain Barrier by Valproic Acid, but Not of Glucose Transporter 1 (GLUT1) or CD98hc

Steinunn Sara Helgudottir , Kasper Bendix Johnsen , Lisa Greve Routhe , Charlotte LM Rasmussen , Maj Schneider Thomsen * , Torben Moos *

Posted Date: 29 April 2024

doi: 10.20944/preprints202404.1939.v1

Keywords: blood-brain barrier; capillary depletion; CD98hc; cell culture; glucose transporter 1; ICP-MS; nanoparticle; transferrin receptor; valproic acid

 doi:10.20944/preprints202404.1939.v1



*Article*

# Upregulation of Transferrin Receptor 1 (TfR1) at the Blood-Brain Barrier by Valproic Acid, but Not of Glucose Transporter 1 (GLUT1) or CD98hc

**Steinunn Sara Helgudóttir [1], Kasper Bendix Johnsen [2], Lisa Juul Routhe [1], Charlotte L.M. Rasmussen [1], Maj Schneider Thomsen [1,*] and Torben Moos [1,*]**

[1] Neurobiology Research and Drug Delivery (NRD), Department of Health Science and Technology, Aalborg University, Denmark
[2] Section for Biotherapeutic Engineering and Drug Targeting, Department of Health Technology, Technical University of Denmark, Lyngby, Denmark
* Correspondence: mst@hst.aau.dk (M.S.T.); tmoos@hst.aau.dk (T.M.)

**Abstract:** Background. Transferrin receptor 1 (TfR1), glucose transporter 1 (GLUT1), and CD98hc are candidates for targeted therapy at the blood-brain barrier (BBB). Our objective was to challenge the expression of TfR1, GLUT1, and CD98hc in brain capillaries by the histone deacetylase inhibitor (HDACi) valproic acid (VPA). Methods. Primary mouse brain capillary endothelial cells (BCECs) and brain capillaries isolated from mice injected intraperitoneally with VPA were examined using RT-qPCR and ELISA. Targeting to the BBB was performed by injecting monoclonal anti-TfR1 (Ri7217)-conjugated gold nanoparticles measured using ICP-MS. Results. In BCECs co-cultured with glial cells, *Tfrc* mRNA expression was significantly higher after 6 h VPA returning to baseline after 24 h. In vivo *Glut1* mRNA expression was significantly higher in males, but not females', receiving VPA, whereas *Cd98hc* mRNA expression was unaffected by VPA. TfR1 increased significantly *in vivo* after VPA, whereas GLUT1 and CD98hc were unchanged. Uptake of anti-TfR1-conjugated nanoparticles was unaltered by VPA in spite upregulated TfR expression. Conclusions. VPA upregulates TfR1 in brain endothelium *in vivo* and *in vitro*. VPA does not increase GLUT1 and CD98hc proteins. The increase in TfR1 does not result in higher anti-TfR1 antibody targetability, suggesting targeting sufficiently occurs with available transferrin receptors without further contribution from accessory VPA-induced TfR1.

**Keywords:** blood-brain barrier; capillary depletion; CD98hc; cell culture; glucose transporter 1; ICP-MS; nanoparticle; transferrin receptor; valproic acid

## 1. Introduction

While denoting the primary obstacle for delivering therapeutics to the brain [1,2], the blood-brain barrier (BBB) is effective in maintaining a stable extracellular environment and prevents unwanted entry of toxins, pathogens, and other harmful molecules [1,3,4]. The BBB is formed by a monolayer of highly specialized brain capillary endothelial cells (BCECs) connected by their intermingling tight junctions, which limit non-specific, paracellular transport [4–8]. Crucial nutrients entering the brain undergo active transport via receptors and transporters expressed on the luminal surface of the BCECs, some of which also have an interest for delivering targeted therapeutics to the brain [5,9].

Limited understanding of expressional patterns and functional regulation of these receptors and transporters remains a challenge for the development of targeted drugs [10]. Drug delivery strategies often target endogenously expressed nutrient transporters delivering e.g. iron (transferrin receptor 1 (TfR1)), glucose (glucose transporter 1 (GLUT1)), or large amino acids (Cluster of Differentiation 98 Heavy Chain (CD98hc). Their availability is under the influence of nutritional demand, age, inflammation, and other pathological processes [11]. The expression of nutrient transporters is probably also challenged by pharmacological treatment, and little is known about e.g. the possible responses of BCECs to treatment with valproic acid (VPA) used for treatment in bipolar disorders

 doi:10.20944/preprints202404.1939.v1



and epilepsia. VPA is thought to induce epigenetic changes by inhibiting histone deacetylase, which further enables acetylation of histones and consequently gene transcription [12].

As we have previously shown that the expression of ferroportin, another iron-transporting molecule (aka SLC40A1 or IREG1), is genetically upregulated in isolated rat BCECs in response to VPA treatment [13], we were led to investigate whether VPA could induce changes in BCECs that would modify the expression of important drug delivery targets, i.e. TfR1, GLUT1, and CD98hc for drug delivery to the brain [14]. We report that VPA treatment in mice upregulates TfR1 at the BBB *in vivo* when examining isolated brain capillaries and *in vitro* when studying isolated primary endothelial cells. In contrast, VPA treatment does not influence the expression of GLUT1 and CD98hc.

## 2. Materials & Methods

The following reagents were purchased from Sigma/Millicell Merck KGaA (Darmstadt, Germany, DE): Insulin transferrin sodium selenite (Cat. no. 11074547001), puromycin (Cat. no. P8833), collagen type IV (Cat. no. C5533), fibronectin (Cat. no. F1141), poly-L-lysine (Cat. no. P6282), hydrocortisone (HC) (Cat. no. H4001), dimethyl sulfoxide (DMSO) (Cat. no. D2650), 8-(4-chlorophenylthio)adenosine 3′,5′-cyclic monophosphate sodium salt (CTP-cAMP) (Cat. no. C3912), 4-(3-butoxy-4-methoxybenzyl)imidazolidin-2-one (RO) (Cat. no. B8279), paraformaldehyde (PFA) (Cat. no. 441244), triton x-100 (Cat. no. X100), 4′,6-diamidino-2-phenylindole dihydrochloride (DAPI), β-mercaptoethanol (Cat. no. M6250), cOmplete Mini, EDTA-free (Cat. no. 11836170001), valproic acid sodium salt (Cat. no. P4543), dextran (MW 60,000 Da), and percoll (Cat. no. P4937).
The following reagents were purchased from Thermo Scientific (Nærum, Denmark, DK): Fetal calf serum (FCS) (Cat. no. 10270), Dulbecco's Modified Eagle Medium consisting of nutrient mixture F-12 (DMEM/F-12) (Cat. no. 31331), DMEM (low glucose) (Cat. no. 21885), DMEM (high glucose) (Cat. no. 31966), trypsin (Cat. no. 15090-46), phosphate-buffered saline (PBS) (Cat. no. SH3025802), rabbit anti-zonula occludens 1 (ZO-1) (Cat. no. 61-7300), Alexa Fluor 488-conjugated goat anti-rabbit IgG (Cat. no. A11034), Alexa Fluor 594-conjugated goat anti-rat IgG (Cat. no. A11007), RevertAid H Minus First Strand cDNA Synthesis Kit (Cat. no. K1652), DNase I enzyme (Cat. no. EN0521), TaqMan Multiplex MasterMix (Cat. no. 4484262), N-PER neuronal protein extraction reagent (Cat. no. 87792), BCA protein assay kit (Cat. no. 23225), TRIzol Plus RNA 41Purification Kit (Cat. no. 12183555). Taqman Fast Advanced MasterMix (Cat.No. 4444963). N-PER neuronal protein extraction reagent (Cat.no 87792). BCA protein essay kit (Cat.no. 23225). TRIzol Plus RNA Purification Kit (Cat.no 12183555). Taqman Probes for CD98hc (Cat.no. 4331182), Glut1 (Cat.no. 4331182, Hprt1 (Cat.no. 4448490).
AllPrep DNA/RNA Mini Kit (Cat. no. 80204) was purchased from Qiagen. Greiner Bio-one Thincert cell culture inserts for 12 well plates with a transparent polyethylene terephthalate (PET) membrane and a pore diameter of 1 μm (Cat. no. 665610) were purchased from In Vitro (Fredensborg, Denmark, DK). Basic fibroblast growth factor (bFGF) (Cat. no. 100-18B) was purchased from PeproTech Nordic (Stockholm, Sweden, SE). Gentamicin sulfate (Cat. no. 17-518Z) was purchased from Lonza Copenhagen (Vallensbaek Strand, Denmark, DK). Plasma-derived bovine serum (PDS) (Cat. no. 60-00-810) was purchased from First Link (Wolverhampton, United Kingdom, UK). Bovine serum albumin (BSA) (Cat. no. EQBAH62) was purchased from Europa Bioproducts (Cambridge, United Kingdom, UK). Fluorescence mounting medium (Cat. no. S3023) was purchased from DAKO (Glostrup, Denmark, DK). Mouse TfR1 ELISA kit (Cat. no. EKM2800) was purchased from BioSite. Isoflurane was purchased from Baxter A/S (Søborg, DK). Collagenase Type II was purchased from Life Technologies. Collagenase/dispase was purchased from Roche.

### *2.1. Isolation of BCECs*

Mice were purchased from Janvier labs (Le Genest-Saint-Isle, FR). Primary brain capillary endothelial cells (BCECs) and pericytes were isolated from eight-week-old C57BL/6 mice as previously described [17,18]. The mice were anesthetized using isoflurane, and their heads submerged in 70 % ethanol before decapitation. The meninges and the brain´s cortical visible white

 doi:10.20944/preprints202404.1939.v1



matter were removed, and the remaining brain tissue was immersed in cold DMEM-F12 medium. They were then digested in DMEM-F12 medium supplemented with collagenase type II and DNase I enzyme at 37°C for 75 minutes in an Incubated mini Shaker (VWR, Søborg, Denmark). Cells were then separated by mixing 20 % bovine serum albumin (BSA) to the solution, followed by a centrifugation step. The pellet containing the microvessel was further digested with collagenase/dispase and DNase I enzyme for 50 minutes at 37°C and separated on a 33 % percoll gradient. Isolated BCECs were maintained in T75 flasks precoated with collagen IV and fibronectin in endothelial medium, which consisted of DMEM-F12 supplemented with 10 % PDS, 0.1 mg/mL ITS, 10 µg/mL gentamicin sulfate, and freshly added 1 ng/mL bFGF. In order to remove pericyte contamination, the BCECs were cultured in media supplemented with 4 µg/ml puromycin for four days [19,20].

*2.2. Isolation of Mixed Glia Cells*

Mixed glial cells were isolated as previously described [18]. The cells were resuspended in DMEM-F12 GlutaMAX medium supplemented with 10 % FCS and 10 µg/mL gentamicin sulfate and seeded in flasks pre-coated with poly-L-lysine. The mixed glial cells were cultured for three weeks in an incubator at 5 % $CO_2$ and 37 °C. The cells were then frozen for later use in DMEM supplemented with 30 % FCS and 7.5 % DMSO. The cells were then seeded in a poly-L-lysine coated 12-well plates and cultured 10 to 14 days until confluence.

*2.3. Construction of In-Vitro Co-Culture BBB Model*

The BCECs were cultured in a $CO_2$ incubator with 5 % $CO_2$ and 95 % $O_2$ at 37 °C. They were then passaged to 12-well hanging culture inserts precoated twice with 1 mg/mL collagen IV and 1 mg/mL fibronectin diluted in Milli-Q water at a density of 100.000 cells/$cm^2$. Once the hanging insert culture contained a fully confluent monolayer of BCECs, they were placed in a 12-well plate containing a population of mixed glia cells, mainly astrocytes. The medium was further supplemented with tight junction-inducing factors, where the medium in the top compartment consisted of 550 nM HC, 250 µM CTP-cAMP, 17.5 µM Ro 20-1724, and the medium in the bottom compartment consisted of a 1:1 mixture of endothelia medium and astrocyte condition medium supplemented with 550 nM HC. The integrity of the BCEC monolayers was evaluated daily by measuring the transendothelial electrical resistance (TEER) using Millicell ERS-2 epithelial volt-ohm meter and STX01 Chopstick Electrodes (Merck Millipore, Hellerup, Denmark, DK). The measured TEER was subtracted from the value of an empty hanging insert containing culture medium, and the value multiplied by the area of the culture insert. The calculated TEER values were presented as mean $\Omega \times cm^2 \pm$ SD. Once the barrier was tight, half of the barriers were treated with 2 mM VPA added directly to the top chamber for 6 h or 24 h.

*2.4. In Vivo Studies*

The mice were processed as shown in Figure 1. Animal experiments were approved by the Animal Experiments Inspectorate under the Danish Ministry of Environment and Food (license number: 2018-15-0201-01550) and performed under European Legislation of Animal Experimentation 2010/63/EU. A total of 48 C57BL/6JRj mice aged 7 weeks, 16 – 24 g, were used for the study. To account for possible gender differences in response to VPA [15,16], both male (n=24) and female (n=24) mice were included. The mice were purchased from Janvier Labs (Le Genest-Saint-Isle, FR) and fed with a commercial diet (Altromin 1324, Brogaarden, Denmark) and had access to food and water ad libitum. They were housed in cages of five with all experimental groups represented in each cage and acclimatized to the local environment (temperature 20 – 22 °C, humidity 40 – 60 %, and light-dark cycle of 12 h) at the animal facility of Aalborg University for 14 days before experiments.

 doi:10.20944/preprints202404.1939.v1



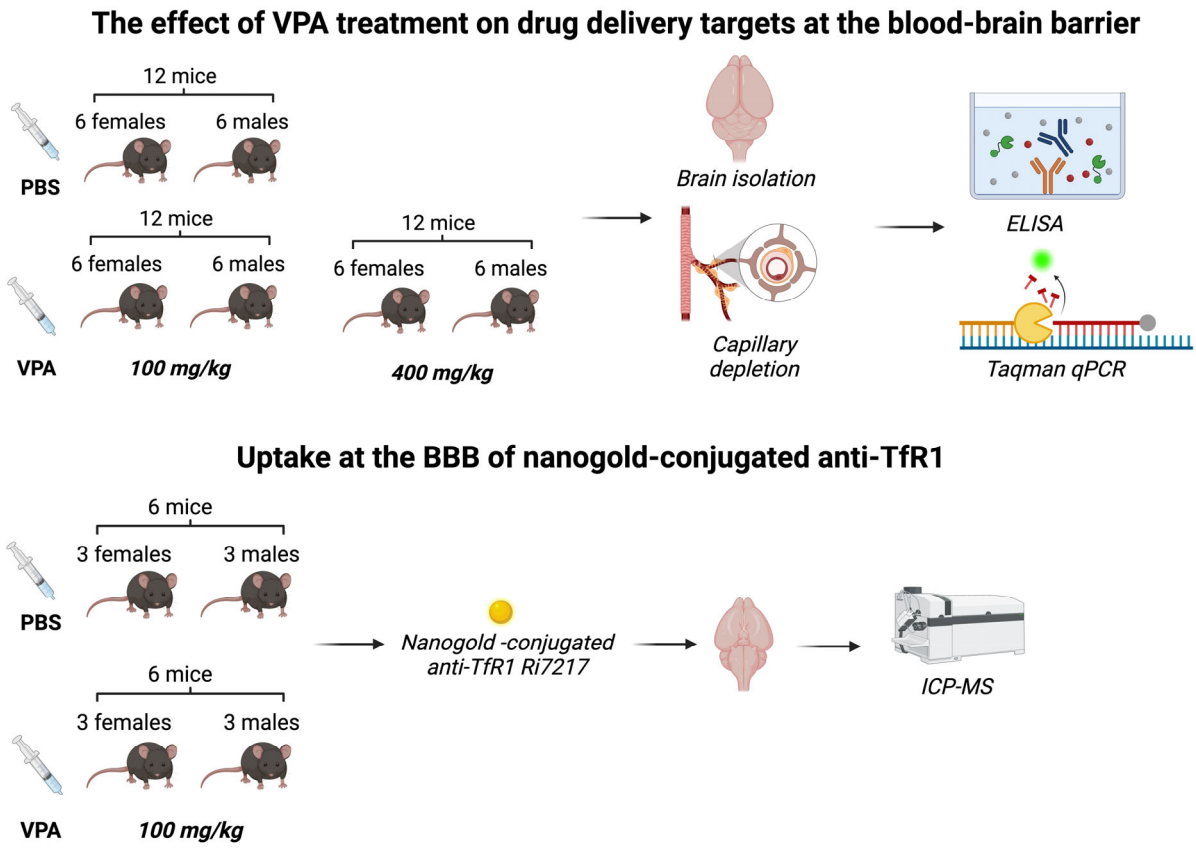


**Figure 1.** Flowchart showing experiments involving living mice.

*2.5. Labeling of Anti-TfR1 Antibodies with 1,4 Nm Gold Nanoparticles*

To estimate the surface availability and transport capability of TfRs at the BBB, we used anti-TfR1 antibodies (clone Ri7217, produced in-house using the hybridoma technique)[23] labelled with 1.4 nm gold nanoparticles (Nanoprobes Inc., Yaphank, NY, US) for high sensitivity detection with inductively-coupled plasma-mass spectrometry. The stock buffer of the anti-TfR1 antibodies (PBS) was exchanged to 0.1 M sodium borate buffer with 2 mM EDTA (pH 8). The buffer-exchanged antibodies were then subjected to thiolation using Traut's reagent (Thermo Scientific, Hvidovre, DK) at a reagent-to-antibody ratio of 10. The solution was allowed to incubate for one hour at room temperature under constant shaking at 500 rpm. The thiolated antibodies were then transferred to an Amicon Ultra spin filter (MW cut-off 30 kDa) (Sigma-Aldrich, Søborg, DK), topped with 5 mL sodium borate buffer, and centrifuged at 4000 g for 20 min at room temperature. The filter-through was discarded, and 5 mL PBS (pH 7.4) was added to the thiolated antibodies. After volume reduction to 50 µL by centrifugation, the thiolated antibodies were transferred to a Protein Lo-Bind Eppendorf tube and stored at 4°C for no more than 30 min. Conjugation of thiolated antibodies to the 1.4 nm gold nanoparticles was performed using Monomaleimide Nanogold Labeling Reagent (Nanoprobes Inc., Yaphank, NY, US) according to the manufacturer's instructions. In short, the lyophilized monomaleide nanoparticles were mixed in 1 mL deionized water and added to 2 mg thiolated antibodies. The air phase was replaced with $N_2$, and the solution was incubated at 4°C overnight. After incubation, the labeled antibodies were separated from unbound gold nanoparticles using gel filtration chromatography on a Superose 6 column (Sigma-Aldrich, Søborg, DK) and stored at 4°C until use.

*2.6. VPA Administration In Vivo*

Mice were randomized into three groups based on body weight. VPA was diluted in sterile PBS and injected intraperitoneally (i.p.) in doses of 100 mg/kg or 400 mg/kg, previously deemed suitable for mice [21]. The control group received injections of sterile PBS. Mice were euthanized 24 h post-

 doi:10.20944/preprints202404.1939.v1



injection. Animals were weighed regularly and monitored for their well-being up until two hours post-injection. They were allowed to recover in a heated cage post-injection. VPA injected in a dose of 100 mg/kg induced a phenotype where the mice became ataxic shortly after administration. In contrast, mice dosed with 400 mg/kg were heavily sedated, which lasted for up to 1 h; after recovery, they presented an ataxic phenotype, but were capable of moving freely in their cage. The adverse effects disappeared within 24 h leading to the full recovery of all mice before termination.

### *2.7. Uptake at the BBB of Nanogold-Conjugated Anti-TfR1 Antibodies*

Mice (n=12) were intravenously injected with nanogold-conjugated anti-TfR1 antibodies (clone Ri7217) 24 h after 100 mg/kg VPA treatment (n=6) or injection of PBS (n=6) (see below). The animals were monitored for 60 minutes after the nanogold-conjugated anti-TfR1 was injected and then euthanized by transcardial perfusion with 20 mL 0.01 M KPBS (pH 7.4) under isoflurane anesthesia; in these mice, brains and peripheral organs of interest were dissected, snap frozen in liquid nitrogen and kept at -80°C until further analysis.

### *2.8. Immunocytochemistry*

Immunocytochemistry was carried out on BCECs to investigate the presence of TfR1 following VPA treatment. Cells were also stained for the tight junction-associated protein, ZO-1 to investigate if the cellular integrity was affected by the treatment. The medium was harvested, and the BCECs were washed in 0.1 M PBS, fixed for 10 min in 4 % PFA and then washed twice in PBS. To block unspecific binding of antibodies, the cells were incubated for 30 min in 3 % BSA and 0.3 % Triton X-100 diluted in 0.1 M PBS. BCECs were incubated for 60 min with anti-TfR1 (clone Ri7217) and ZO-1 diluted 1:200 in a blocking buffer. The cells were subsequently washed twice in a washing buffer to remove any unbound primary antibodies. The cells were then incubated for 60 min with secondary antibodies Alexa Flour 594-conjugated goat anti-rat and Alexa Flour 488-conjugated goat anti-rabbit diluted 1:200 in blocking buffer followed by washing. The nuclei were stained with DAPI for 5 min diluted 1:1000 in PBS. Cells were mounted onto slides using DAKO fluorescent mounting medium and examined using an AxioObserver Z1 fluorescence microscope equipped with an ApoTome.2 and Axiocam MR camera under a Plan-Apochromat 40x/1.3 NA oil DIC objective. Images were corrected for brightness and contrast using the ImageJ software.

### *2.9. Capillary Depletion*

Brain capillary isolation was performed to separate the brain capillaries from the remaining brain tissue. Brains from mice dosed with 100 mg/kg, 400 mg/kg VPA, or PBS were dissected, and the right cerebral hemisphere was sampled and transferred to a Dounce homogenizer. Ice-cold capillary depletion buffer [22] was added, and the brains were homogenized by six strokes, followed by mixing with ice-cold 30% dextran and further homogenization with six strokes. The homogenate was transferred into a 15 mL Falcon tube and centrifuged at 5,400 g for 40 min at 4°C. The capillary and supernatant fractions were carefully separated and stored at –80°C until further analyses.

### *2.10. Quantification of Tissue Gold Content*

The gold content in tissue samples was analyzed using inductively-coupled plasma-mass spectrometry. The samples were digested in aqua regia overnight at 65 °C followed by dilution in deionized water containing 0.5 ppb iridium (Fluka, Sigma-Aldrich, Brøndby, DK). Immediately before analysis, the samples were diluted in 2 % HCl containing 0.5 ppb iridium, after which they were analyzed on an iCAP Q ICP-MS system (Thermo Scientific, Hvidovre, DK) fitted with an ASX-520 AutoSampler and a Neclar ThermoFlex 2500 chiller. Performance on the instrument was ensured by calibration using TUNE B iCAP Q element mixture (Thermo Scientific, Hvidovre, DK). A standard curve was generated by serial dilution of an analytical grade gold standard solution to obtain the gold concentration in each sample (Fluka, Sigma-Aldrich, Brøndby, DK). Measurement of the iridium concentration was used as an internal standard to ensure similar analysis of all samples.

 doi:10.20944/preprints202404.1939.v1



*2.11. Probe-Based RT-qPCR*

The purification of RNA from BCECs was carried out using the AllPrep DNA/RNA Mini kit following the manufacturer´s protocol. RNA concentrations were assessed using DS-11 FX Spectrophotometer/Fluorometer (DeNovix, USA). A total of 150 ng RNA was treated with DNAse I enzyme to remove any potential genomic contamination, mixed with nuclease free water, 10x reaction buffer and incubated for 30 minutes in a T100 Thermal cycler (Bio-rad) at 37°C. All samples were then treated with Ethylenediaminetetraacetic acid (EDTA) for 10 minutes at 65°C to stop the reaction. Complementary DNA was generated using the RevertAid H Minus First Strand cDNA Synthesis Kit, which consisted of random hexamer primer, oligo primer, 10 mM dNTP, 5x reaction buffer and nuclease free water. This was mixed with Maxima H Enzyme mix and 100 ng of DNase treated RNA and the samples run in the thermal cycler using the following thermal profile: 10 minutes at 25°C, 15 minutes at 50°C and 5 minutes at 85°C. The RT-qPCR was carried out by preparing a mastermix containing the TaqMan Multiplex MasterMix and Taqman primer/probe for *Glut1*, *CD98hc*, *Tfrc*, *Hprt1*, then adding 1.7 ng sample in each well. The samples were run on QuantStudio 6 Flex Real-Time PCR System (Thermo Fisher Scientific) with the thermal profile: 50°C for 2 min, 95°C for 20 seconds, followed by 40 cycles of 95°C for 1 second and 60°C for 20 seconds. After the run, samples were cooled down to 20°C. The relative mRNA expression was calculated using the ΔΔCT method, and the expression was normalized to *Hprt1* expression where PBS-injected mice served as the reference sample.

*2.12. Elisa*

Enzyme-linked immunosorbent assay (ELISA) was used to measure the amount of TfR1, GLUT1, and CD98hc in isolated brain capillaries after PBS or VPA treatment to evaluate these proteins at the level of the BBB [24]. To account for varying protein concentrations in each sample, the total protein concentration was measured using a BCA protein assay kit as previously described [13]. Each sample was lysed using 90 µL N-PER™ Neuronal protein extraction buffer supplemented with cOmplete Mini protease inhibitor. The samples were lysed on ice for 10 min and spun down at 14,000 g for 10 min at 4°C and the supernatant collected. Samples were diluted 1:10 in sample buffer and analyzed using sandwich-ELISA for mouse TfR1, GLUT1, and CD98hc according to the manufacturer's protocol. The absorbance was read at 450 nm using an Enspire Plate Reader from Perkin Elmer, and the concentration was calculated using a standard curve and normalized to the total protein concentration of each sample.

*2.13. Statistical Analysis*

The relative gene expression of *Tfrc, Glut1*, and *Cd98hc* mRNA from mice and isolated BCECs was calculated according to the ΔΔCT method. All data was checked for normal distribution before performing statistical analysis. The results were analyzed using one-way ANOVA with Dunnett´s multiple comparisons test in GraphPad Prism 9. When investigating the difference in mRNA expression between male and female mice, a two-way ANOVA with the Holm-Sidak multiple comparisons test was used. ELISA data on TfR1, GLUT1, and CD98Hc in brain capillaries was analyzed by one-way ANOVA with Dunnett´s multiple comparisons test. The luminal binding of Nanogold-conjugated anti-TfR1 antibodies was analyzed by unpaired t-test. Significance levels were *p = 0.01–0.05, **p = 0.001–0.01, ***p = 0.0001–0.001, and ****p < 0.0001.

**3. Results**

*3.1. VPA Administration Upregulates Tfrc in BCECs In Vitro*

To evaluate the effects of VPA on the expression of important drug delivery targets, BCECs co-cultured with mixed glial cells were treated with 2mM VPA for 6 h or 24 h (Figure 2A). The integrity of the barriers was evaluated via measurement of TEER followed by immunolabeling of the tight junction-associated protein, ZO-1. The TEER was unaffected by VPA treatment both after 6 h and 24

 doi:10.20944/preprints202404.1939.v1



h (Figure 2B). The expression and subcellular distribution of ZO-1 were similar between the control barriers and the barriers treated with VPA for 24 h (Figure 3). Having established that the VPA treatment did not affect the integrity of the *in vitro* barriers, we then analyzed the effect of VPA treatment on the expression profiles of *Tfrc*, *Glut1*, and *Cd98hc*. The mRNA expression of *Tfrc* was significantly higher after VPA treatment for 6 h, and the expression level returned to baseline after 24 h (Figure 2C). Conversely, the mRNA expression of *Glut1* and *Cd98hc* was unaffected by VPA treatment (Figs. 2D-E). VPA did not only increase the gene expression of *Tfrc.* By visual inspection, the TfR1 protein was particularly high in the perinuclear region of the BCECs compared to the control BCECs suggestive of an increased presence of TfR1 in the granular endoplasmic reticulum (Figure3).

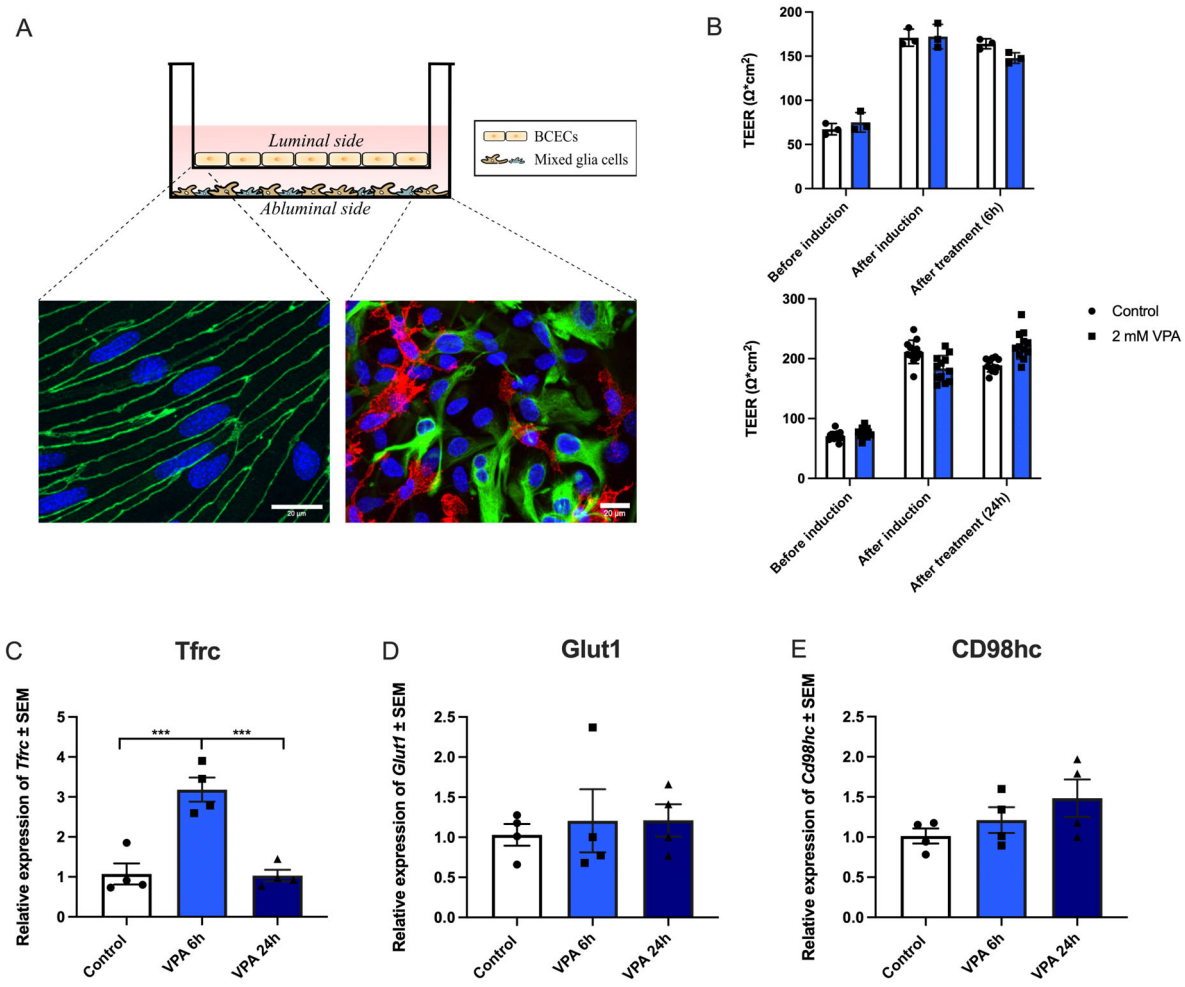


**Figure 2. *In vitro* experiments addressing the effects of valproic acid (VPA) on gene expression of *Tfrc*, *Glut1*, and *Cd98hc*.** (A) Transwell system illustrating a non-contact co-culture system where brain capillary endothelial cells (BCECs) are cultured on hanging inserts, making up the luminal side of the barrier. The mixed glial cells are cultured in the bottom of the well, making up the abluminal side of the barrier. The immunocytochemistry illustrations display BCECs (on the left) stained with ZO-1 and Dapi, and the mixed glia culture (on the right) stained for GFAP (green) to identify astrocytes and Cd11b (red) to identify microglia, as well as Dapi. The scale bar is 20 µm. (B) The transendothelial electrical resistance (TEER) was investigated before and after tight junction induction, as well as treatment with 2mM VPA for 6 (n=3) and 24 (n=12) hours (h). The tightness of the barrier remains intact after treatment with VPA for at least 24 h. (C-E) Expression of *Tfrc, Glut1,* and *CD98hc* mRNA. (C) The expression of *Tfrc* in BCECs increases after 6 h of treatment with VPA and returns to baseline after 24 h. In contrast, there are no changes in expression of *Glut1* (D) or *CD98hc* (E) following VPA treatment. Gene expression was analyzed using one-way ANOVA with Dunnett´s multiple comparisons test. Data (n=4) are shown as mean ±SEM, ***p =0.0001–0.001.

 doi:10.20944/preprints202404.1939.v1



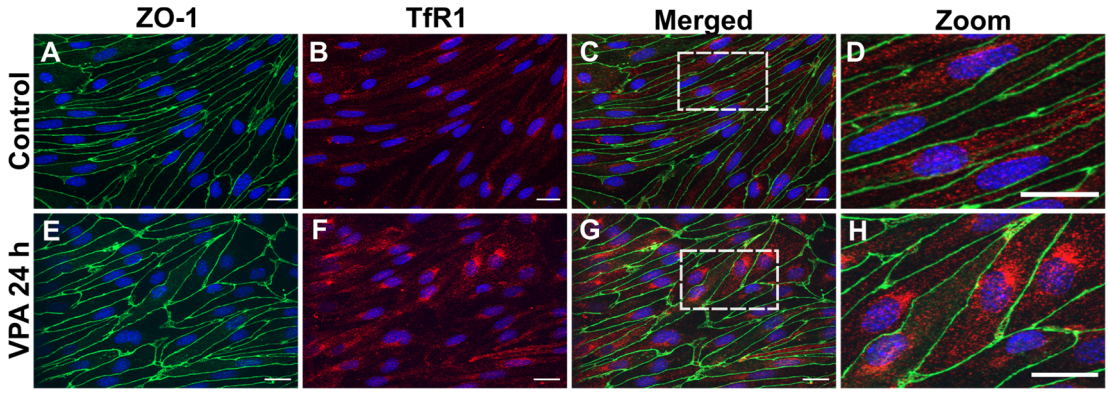


**Figure 3. TfR1 protein in cultured brain endothelial cells (BCECs) after valproic acid (VPA) treatment.** Zonula occludens (ZO-1; green) and TfR1 (red) detection using immunocytochemistry in BCECs co-cultured with mixed glial cells and treated with PBS (A-D) or 2 mM VPA (E-H). The tight junction protein ZO-1 remains highly expressed despite treatment with VPA (compare A with E). Morphologically, the increased expression of *Tfrc* (Figure 2) translates to increased TfR1 protein (compare B and F). When shown in high magnification (D and H), it is evident that the TfR1 protein is highly expressed after VPA treatment revealing a perinuclear distribution, probably reflecting a higher abundance in the granular endoplasmic reticulum. The nuclei are stained with DAPI (blue). Scale bar: 20 μm.

### *3.2. VPA Induces TfR1 Expression In Vivo*

We next wanted to investigate if VPA had the same effects on gene and protein expression of TfR1, GLUT1, and CD98hc in living animals as in the *in vitro* cultured BCECs. Analyzing the isolated brain capillaries from PBS, 100 mg/kg VPA, and 400 mg/kg VPA treated animals, the expression of *Tfrc* was unaltered between treatment groups 24 h post-injection (Figure 4A) with no difference in expression between male and female mice (Figure 4B). In contrast, the TfR1 protein in capillaries increased significantly after treatment with both 100 mg/kg and 400 mg/kg VPA (Figure 4C). The TfR1 level ranged from 1.5 to 3.7 ng/μg protein and was not impacted by the gender of the animals (Figure 4D).

 doi:10.20944/preprints202404.1939.v1



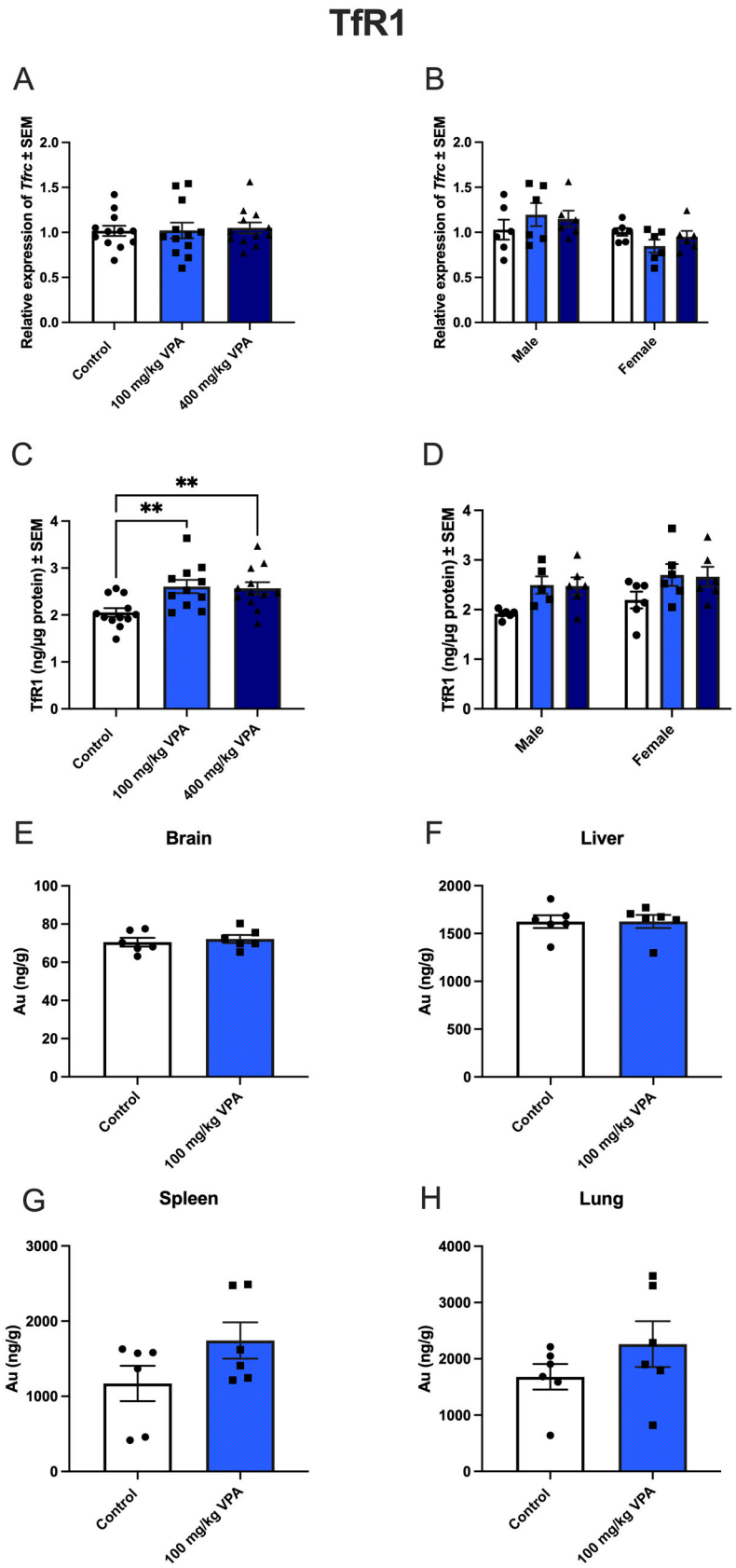


**Figure 4.** *Tfrc* gene expression (A,B) and TfR1 protein (C,D) after valproic acid (VPA) treatment *in vivo*, and uptake of gold-labeled TfR1-targeted antibodies (E-H). A,B) *Tfrc* gene expression in capillary depleted brain extracts from mice treated with PBS, 100 mg/kg VPA, or 400 mg/kg VPA for 24 hours. A) Total cohort, B) Separation by sex. (Males, n=6; Females, n=6 for each treatment group). Gene

 doi:10.20944/preprints202404.1939.v1



expression is analyzed using one-way ANOVA with Dunnett´s multiple comparisons and when investigating the difference in mRNA expression between male and female mice, a two-way ANOVA with the Holm-Sidak multiple comparisons test is used. Data (n=6-12) are shown mean ± SEM. No differences are observed in *Tfrc* mRNA expression in the group of all animals (A) or after division by sex (B). C) When analyzed for TfR1 protein in isolated capillaries, both 100 mg (n=12) and 400 mg (n=12) VPA treatment for 24 hours significantly increased TfR1 protein with upregulation in both male and female mice (D). One-way ANOVA with Dunnett's multiple comparisons test was used for statistical analysis. **p = 0.001–0.01. Data (n=11-12) are depicted as mean ± SEM. E-H) Uptake of gold-labeled TfR1-targeted antibodies. Uptake of TfR1 -conjugated gold 1 nm nanoparticles in brain, liver, spleen, and lung of untreated and VPA-treated mice. The uptake of TfR1 antibody-conjugated gold nanoparticles, determined based on the content of gold in the isolated capillaries and brain fraction using ICP-MS, is similar in the brain (E), and hepatocytes of the liver (F) in control and VPA-injected mice. The uptake in the spleen (G) and lung (H) seems to increase slightly although differences are insignificant. Statistical difference between control and VPA-treated animals is analyzed with an unpaired t-test, and each point represents data from a single mouse (n=6), and the data are depicted as mean ± SEM.

### *3.3. Uptake of Gold-Labeled Anti-TfR1 Antibodies*

Next, we wanted to study, whether the increased TfR1 protein in brain capillaries induced by VPA could be quantitatively reflected by increased uptake of gold-labeled anti-TfR1 antibodies. We administered the antibodies intravenously at a dose of 1 mg/kg to VPA-treated (100 mg/kg for 24 hours) and control male mice and allowed them to circulate for 60 min. Using ICP-MS-based quantification of the gold content, the accumulation in brain capillaries was non-significant suggesting that VPA treatment did not improve the uptake of the anti-TfR1 antibodies despite increased TfR1 (Figure 4E). Similarly, the uptake of the gold-labeled anti-TfR1 antibodies in liver, lung, and spleen, organs in where TfR1 is mainly expressed in hepatocytes, and macrophages was unaltered (Figs. 4F-H).

### *3.4. VPA Increases Glut1 mRNA in Male, but Not in Female Mice*

The relative gene expression of *Glut1* in isolated capillaries was unaffected by treatment with 100 mg/kg and 400 mg/kg VPA after 24 hours (Figure 5A). However, gender-related differences were observed as male mice treated with 400 mg/kg VPA for 24 hours significantly upregulated their expression of *Glut1* compared to the PBS treated male mice (Figure 5B). The increased expression of *Glut1* among the 400 mg/kg VPA treated male mice was not reflected in the GLUT1 protein (Figure 4D), as GLUT1 protein content was unchanged in all treatment groups (Figs. 5C-D). The content of GLUT1 protein ranged 0.4-1.8 ng/ µg protein.

 doi:10.20944/preprints202404.1939.v1



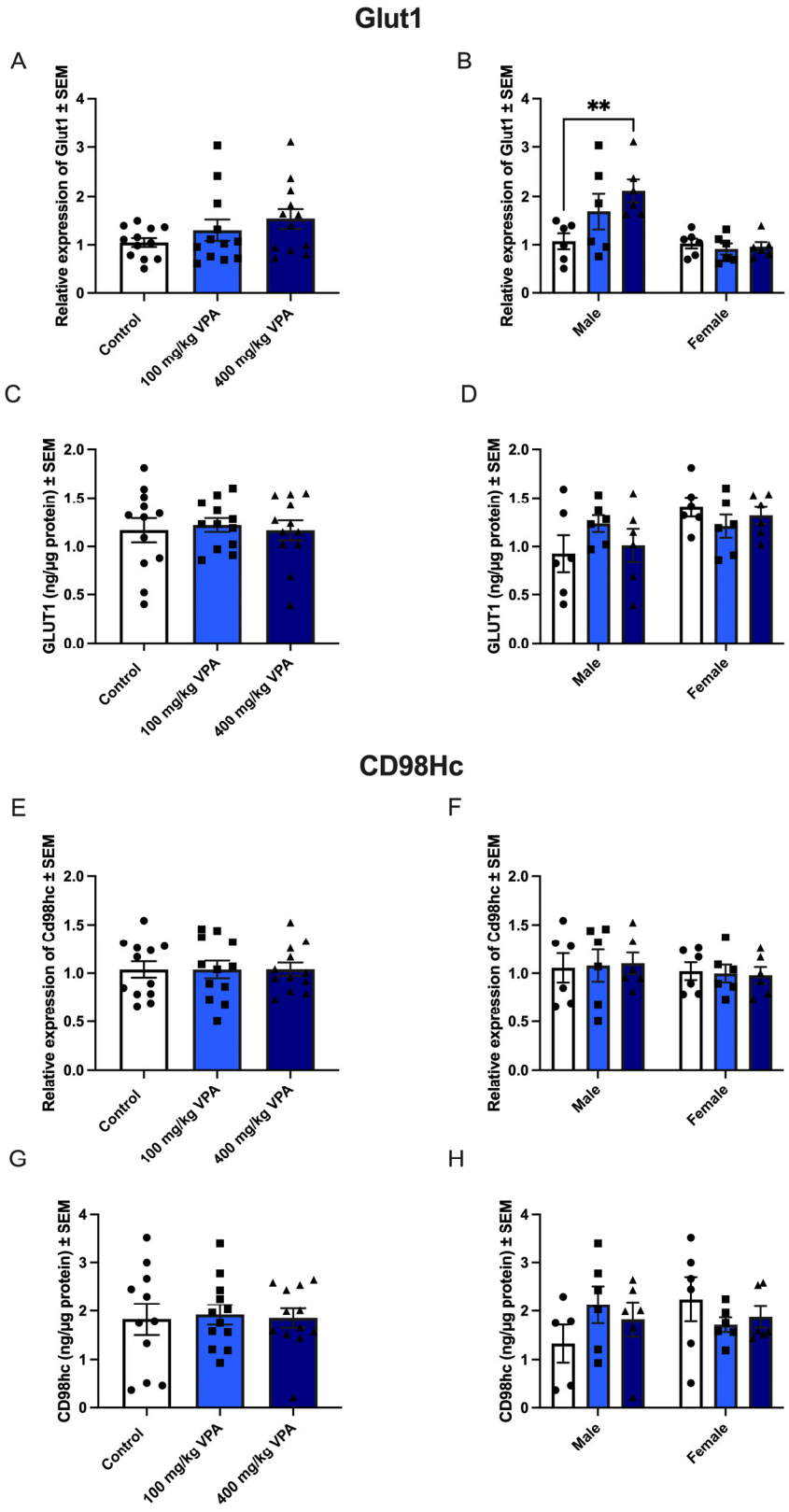


**Figure 5.** GLUT1 (upper panel) and CD98hc (lower panel) gene and protein expression in isolated brain capillaries after valproic acid (VPA) treatment. Upper panel. (A) Relative *Glut1* gene expression in brain capillaries from mice treated with PBS (n=12), 100 mg/kg VPA (n=12), or 400 mg/kg VPA (n=12) for 24 hours. (B) The *Glut1* expression profile is separated based on sex (males n=6 and females n=6 for each treatment group). No differences are observed in *Glut1* expression in the group of all animals (A), but significance is seen in the group of males when separated by sex (B) **p =0.001–0.01.

 doi:10.20944/preprints202404.1939.v1



Gene expression was analyzed using one-way ANOVA with Dunnett´s multiple comparisons and when investigating the difference in gene expression between male and female mice, a two-way ANOVA with the Holm-Sidak multiple comparisons test was used. Data (n=6-12) are shown mean ± SEM, **p =0.001–0.01. (C-D) When analyzed for GLUT1 protein in isolated capillaries from controls (n=12) and mice treated with 100 mg/kg VPA (n=12) and 400 mg/kg VPA (n=12), no significant difference in GLUT1 is seen nor when separated by sex (D). One-way ANOVA with Dunnett's multiple comparisons test was used for statistical analysis. Data (n=12) are depicted as mean ± SEM. (E-F) Relative *Cd98hc* gene expression in brain capillaries from mice treated with PBS (n=12), 100 mg/kg VPA (n=12), or 400 mg/kg VPA (n=12) for 24 hours. The *Cd98hc* expression profile was separated based on sex (males n=6 and females n=6 for each treatment group). A change in gene expression is analyzed using one-way ANOVA with Dunnett´s multiple comparisons and when investigating the difference in gene expression between male and female mice, a two-way ANOVA with the Holm-Sidak multiple comparisons test was used. No differences are observed in *Cd98hc* expression in the group of all animals (A), nor when separated by sex (B). Data (n=6-12) are shown mean ± SEM. (G-H) CD98hc protein in capillaries of mice injected with PBS (n=12) or VPA in concentrations of 100 mg/kg (n=12) or 400 mg/kg (n=12) allowed to circulate for 24 hours. The VPA treatment does not lead to significant changes in the CD98hc protein content. One-way ANOVA with Dunnett's multiple.

### *3.5. CD98hc expression Is not Affected by VPA Treatment*

The relative gene expression of *CD98hc* was unaltered between the PBS and the VPA-treated mice, and no difference was observed between male and female mice (Figs. 5E-H). CD98hc protein was present in capillaries, ranging from 0.4-3.7 ng/ µg protein.

## 4. Discussion

Targeting nutrient receptors and transporters, which are highly expressed at the BBB is of interest for delivery of large therapeutics to the brain [25]. The intriguing possibility of pharmacologically increasing the expression of TfR1, GLUT1, or CD98hc on BCECs in a manner that could increase the availability of targetable molecules inspired this study.

VPA is known to interact at the level of the BBB, e.g. VPA prevents BBB disruption after subarachnoid hemorrhage [26] and intracerebral hemorrhage [27], and it lessens BBB disruption after transient focal cerebral ischemia [28]. VPA inhibits the histone deacetylation process, thereby ensuring the accessibility of transcription factors to the chromatin, which increases gene transcription of multiple genes and is therefore not specific to the aforementioned targets [12,28,29]. VPA was initially approved as an anti-epileptic drug, but its ability to inhibit HDAC could explain the increase in TfR1 observed in the current study [30].

TfR1 remains the most studied receptor for targeting the BBB. The reason for its popularity is that TfR1 is only expressed on BCECs and not on other endothelial cells in the body [31], which leads to a preferential cerebral accumulation of TfR1 targeted molecules [31,32]. TfR1 promotes the uptake of transferrin-bound iron, which is an essential co-factor in multiple physiological functions such as cell division, DNA synthesis, and oxygen transport [33–37]. We found that VPA treatment increases the expression of *Tfrc* significantly after 6 hours *in vitro*, reaching an expression of three times greater than the controls and that the expression was back to baseline after 24 hours of treatment. To examine whether this effect was species-specific, we have conducted similar experiments in the rat where *Tfrc* increased 2.5-fold following VPA treatment [38].

The relative gene expression of *Tfrc* was also investigated in purified brain capillaries from mice treated with VPA for 24 hours. However, there was no indication of altered expression of *Tfrc* 24 h post-injection. It remains to be answered whether the expression of *Tfrc* is regulated by post-transcriptional mechanisms rather than regulation of mRNA synthesis [39], meaning that in conditions with e.g. deprivation of nutritional iron supply, cells upregulate TfR1 protein by increasing translation of its mRNA.

 doi:10.20944/preprints202404.1939.v1



In BCECs, the content of TfR1 is particularly high during the development of the brain and ceases with increasing postnatal age [40–42]. In the rat, this was also reflected in a developmentally higher uptake of iron-containing transferrin and a monoclonal antibody (OX26) targeting TfR1 following intravenous injection [43]. The current study suggests that VPA also leads to increased post-translational regulation of TfR1 in BCECs. Prior studies in isolated porcine BCECs suggest that BCECs harbor a significant spare pool of transferrin receptors that can be mobilized when needed as occurring in conditions with cerebral iron deficiency [44,45]. The present study examining adult mice did not record an increased uptake of 1,4 nm gold-conjugated anti-transferrin receptor antibodies despite a higher content of TfR1 following VPA treatment. This absence suggests that the quantity of functionally available TfR1 molecules contributing to cellular uptake of the targeted anti-TfR1 antibody remained unaltered in BCECs following VPA treatment. This also suggests that the observed increase in TfR1 protein in BCECs following VPA treatment is attributed to an enlargement of the intracellular TfR1 pool. Possibly the BCECs' uptake of iron-transferrin and targeted antibodies in adults operates primarily via mobilization of this intracellular pool of spare TfR1, which could get contribution from the pharmacologically enhanced TfR1 protein.

The overall expression of GLUT1 or CD98hc in the current study is not being affected by VPA treatment. GLUT1 in the brain is selectively confined to BCECs and is additionally among the most abundant proteins in BCECs [46–48]. GLUT1 is regulated in accordance with the brain's metabolic needs, and a reduction has been observed in Alzheimer´s disease [49–51]. However, when dividing the animals to groups dependent on gender, there was a significantly higher expression of *Glut1* in the brains of male mice that had been treated with VPA, but not in females. These results underscore the importance of incorporating both male and female mice in experiments. Why male mice seem to be more affected by the acetylation status of GLUT1 promotor at the BBB is unknown.

Manipulation of histone acetylation affects around 2% of genes [12], and CD98hc seems to fall into the 98% of genes unaffected by acetylation status. CD98hc has been verified as a strong candidate for pharmacological targeting to the BBB [52] where various delivery platforms utilizing its high and selective expression are being investigated. CD98hc is an intracellular amino acid transporter and integrin signaling enhancer[14] and among the most highly expressed transcripts in human and mouse brain capillaries [25,32,53], which is in agreement with the high CD98hc protein detected in the ELISA of the present study.

## 5. Conclusions

The current study showed that it is possible to upregulate TfR1 protein in BCECs utilizing the histone deacetylase inhibitor VPA. Upregulation of protein was not seen for GLUT1 or CD98hc, two other major molecular targets for drug delivery through the BBB. The increase in TfR1 protein at the BBB was not accompanied by higher targetability of a specific anti-TfR1 targeted monoclonal antibody, which suggests that targeted delivery to TfR1 engages with already available transferrin receptor without further aid of VPA-induced TfR1.

**Acknowledgments:** We thank Merete Fredsgaard and Hanne Krone Nielsen, Aalborg University, Denmark, for their excellent technical assistance.

**Funding:** The present study has been supported by the Lundbeck Foundation Research Initiative on Brain Barriers and Drug Delivery (Grant no. R155-2013-14113, Torben Moos), the Danish Multiple Sclerosis Society (Grant no. A38230, Torben Moos), Parkinsonforeningen (Torben Moos) and Svend Andersen Fonden (Torben Moos).

## References

1. Abbott, N.J. Blood–Brain Barrier Structure and Function and the Challenges for CNS Drug Delivery. *Journal of Inherited Metabolic Disease* **2013**, *36*, 437–449, doi:10.1007/s10545-013-9608-0.
2. Pardridge, W.M. Blood-Brain Barrier and Delivery of Protein and Gene Therapeutics to Brain. *Frontiers in Aging Neuroscience* 2020, *11*.
3. Mills, E.; Dong, X.-P.; Wang, F.; Xu, H. Mechanisms of Brain Iron Transport: Insight into Neurodegeneration and CNS Disorders. *Future medicinal chemistry* **2010**, *2*, 51–64, doi:10.1021/ac901991x.

4. Abbott, N.J.; Rönnbäck, L.; Hansson, E. Astrocyte–Endothelial Interactions at the Blood–Brain Barrier. *Nature Reviews Neuroscience* **2006**, *7*, 41–53, doi:10.1038/nrn1824.
5. Abbott, N.J.; Patabendige, A.A.K.; Dolman, D.E.M.; Yusof, S.R.; Begley, D.J. Structure and Function of the Blood-Brain Barrier. *Neurobiology of Disease* **2010**, *37*, 13–25, doi:10.1016/j.nbd.2009.07.030.
6. Daneman, R.; Prat, A. The Blood–Brain Barrier. *Cold Spring Harbor Perspectives in Biology* **2015**, *7*, doi:10.1101/cshperspect.a020412.
7. Greene, C.; Hanley, N.; Campbell, M. Claudin-5: Gatekeeper of Neurological Function. *Fluids and barriers of the CNS* **2019**, *16*, 3, doi:10.1186/s12987-019-0123-z.
8. Reese, T.S.; Karnovsky, M.J. Fine Structural Localization of a Blood-Brain Barrier to Exogenous Peroxidase. *The Journal of cell biology* **1967**, *34*, 207–217, doi:10.1083/jcb.34.1.207.
9. Zlokovic, B. V. The Blood-Brain Barrier in Health and Chronic Neurodegenerative Disorders. *Neuron* **2008**, *57*, 178–201, doi:10.1016/j.neuron.2008.01.003.
10. Kevadiya, B.D.; Ottemann, B.M.; Thomas, M. Ben; Mukadam, I.; Nigam, S.; McMillan, J.E.; Gorantla, S.; Bronich, T.K.; Edagwa, B.; Gendelman, H.E. Neurotheranostics as Personalized Medicines. *Advanced Drug Delivery Reviews* **2018**, doi:10.1016/j.addr.2018.10.011.
11. Moura, R.P.; Martins, C.; Pinto, S.; Sousa, F.; Sarmento, B. Blood-Brain Barrier Receptors and Transporters: An Insight on Their Function and How to Exploit Them through Nanotechnology. *Expert Opinion on Drug Delivery* 2019, *16*, 271–285.
12. Bhatti, U.F.; Williams, A.M.; Georgoff, P.E.; Alam, H.B. The 'Omics' of Epigenetic Modulation by Valproic Acid Treatment in Traumatic Brain Injury—What We Know and What the Future Holds. *Proteomics - Clinical Applications* 2019, *13*.
13. Helgudottir, S.S.; Routhe, L.J.; Burkhart, A.; Jønsson, K.; Pedersen, I.S.; Lichota, J.; Moos, T. Epigenetic Regulation of Ferroportin in Primary Cultures of the Rat Blood-Brain Barrier. *Molecular Neurobiology* **2020**, *57*, 3526–3539, doi:10.1007/s12035-020-01953-y.
14. Zuchero, Y.J.Y.; Chen, X.; Bien-Ly, N.; Bumbaca, D.; Tong, R.K.; Gao, X.; Zhang, S.; Hoyte, K.; Luk, W.; Huntley, M.A.; et al. Discovery of Novel Blood-Brain Barrier Targets to Enhance Brain Uptake of Therapeutic Antibodies. *Neuron* **2016**, *89*, 70–82, doi:10.1016/j.neuron.2015.11.024.
15. Long, Z.; Zeng, Q.; Wang, K.; Sharma, A.; He, G. Gender Difference in Valproic Acid-Induced Neuroprotective Effects on APP/PS1 Double Transgenic Mice Modeling Alzheimer's Disease. *Acta Biochimica et Biophysica Sinica* **2016**, *48*, 930–938, doi:10.1093/abbs/gmw085.
16. Ibarra, M.; Vázquez, M.; Fagiolino, P.; Derendorf, H. Sex Related Differences on Valproic Acid Pharmacokinetics after Oral Single Dose. *Journal of Pharmacokinetics and Pharmacodynamics* **2013**, *40*, 479–486, doi:10.1007/s10928-013-9323-3.
17. Thomsen, M.S.; Birkelund, S.; Burkhart, A.; Stensballe, A.; Moos, T. Synthesis and Deposition of Basement Membrane Proteins by Primary Brain Capillary Endothelial Cells in a Murine Model of the Blood-Brain Barrier. *Journal of Neurochemistry* **2017**, *140*, 741–754, doi:10.1111/jnc.13747.
18. Thomsen, M.S.; Humle, N.; Hede, E.; Moos, T.; Burkhart, A.; Thomsen, L.B. The Blood-Brain Barrier Studied in Vitro across Species. *PloS one* **2021**, *16*, doi:10.1371/JOURNAL.PONE.0236770.
19. Perrière, N.; Demeuse, P.H.; Garcia, E.; Regina, A.; Debray, M.; Andreux, J.P.; Couvreur, P.; Scherrmann, J.M.; Temsamani, J.; Couraud, P.O.; et al. Puromycin-Based Purification of Rat Brain Capillary Endothelial Cell Cultures. Effect on the Expression of Blood-Brain Barrier-Specific Properties. *Journal of Neurochemistry* **2005**, *93*, 279–289, doi:10.1111/j.1471-4159.2004.03020.x.
20. Calabria, A.R.; Weidenfeller, C.; Jones, A.R.; De Vries, H.E.; Shusta, E. V. Puromycin-Purified Rat Brain Microvascular Endothelial Cell Cultures Exhibit Improved Barrier Properties in Response to Glucocorticoid Induction. *Journal of Neurochemistry* **2006**, *97*, 922–933, doi:10.1111/j.1471-4159.2006.03793.x.
21. Chaliha, D.; Albrecht, M.; Vaccarezza, M.; Takechi, R.; Lam, V.; Al-Salami, H.; Mamo, J. A Systematic Review of the Valproic-Acid-Induced Rodent Model of Autism. *Developmental neuroscience* **2020**, *42*, 12–48, doi:10.1159/000509109.
22. Johnsen, K.B.; Bak, M.; Kempen, P.J.; Melander, F.; Burkhart, A.; Thomsen, M.S.; Nielsen, M.S.; Moos, T.; Andresen, T.L. Antibody Affinity and Valency Impact Brain Uptake of Transferrin Receptor-Targeted Gold Nanoparticles. *Theranostics* **2018**, *8*, 3416–3436, doi:10.7150/thno.25228.
23. Kucharz, K.; Kristensen, K.; Johnsen, K.B.; Lund, M.A.; Lønstrup, M.; Moos, T.; Andresen, T.L.; Lauritzen, M.J. Post-Capillary Venules Are the Key Locus for Transcytosis-Mediated Brain Delivery of Therapeutic Nanoparticles. *Nature communications* **2021**, *12*, doi:10.1038/S41467-021-24323-1.
24. Hill, J.J.; Haqqani, A.S.; Stanimirovic, D.B. Proteome of the Luminal Surface of the Blood–Brain Barrier. *Proteomes* **2021**, *9*, doi:10.3390/PROTEOMES9040045.
25. Moos, T.; Thomsen, M.S.; Burkhart, A.; Hede, E.; Laczek, B. Targeted Transport of Biotherapeutics at the Blood-Brain Barrier. *Expert opinion on drug delivery* **2023**, *20*, 1823–1838, doi:10.1080/17425247.2023.2292697.
26. Ying, G.; Jing, C.; Li, J.; Wu, C.; Yan, F.; Chen, J.; Wang, L.; Dixon, B.J.; Chen, G. Neuroprotective Effects of Valproic Acid on Blood-Brain Barrier Disruption and Apoptosis-Related Early Brain Injury in Rats Subjected to Subarachnoid Hemorrhage Are Modulated by Heat Shock Protein 70/Matrix

Metalloproteinases and Heat Shock Protein 70/AKT Pathways. *Neurosurgery* **2016**, *79*, 286–295, doi:10.1227/NEU.0000000000001264.
27. Zhao, W.; Zhao, L.; Guo, Z.; Hou, Y.; Jiang, J.; Song, Y. Valproate Sodium Protects Blood Brain Barrier Integrity in Intracerebral Hemorrhage Mice. *Oxidative Medicine and Cellular Longevity* **2020**, *2020*, doi:10.1155/2020/8884320.
28. Hwang, J.Y.; Aromolaran, K.A.; Zukin, R.S. The Emerging Field of Epigenetics in Neurodegeneration and Neuroprotection. *Nature Reviews Neuroscience* 2017, *18*, 347–361.
29. Bowman, G.D.; Poirier, M.G. Post-Translational Modifications of Histones That Influence Nucleosome Dynamics. *Chemical Reviews* 2015, *115*, 2274–2295.
30. Ornoy, A.; Becker, M.; Weinstein-Fudim, L.; Ergaz, Z. S-Adenosine Methionine (SAME) and Valproic Acid (VPA) as Epigenetic Modulators: Special Emphasis on Their Interactions Affecting Nervous Tissue during Pregnancy. *International Journal of Molecular Sciences* 2020, *21*.
31. Jefferies, W.A.; Brandon, M.R.; Hunt, S. V.; Williams, A.F.; Gatter, K.C.; Mason, D.Y. Transferrin Receptor on Endothelium of Brain Capillaries. *Nature* **1984**, *312*, 162–163, doi:10.1038/312162a0.
32. Zhang, W.; Liu, Q.Y.; Haqqani, A.S.; Leclerc, S.; Liu, Z.; Fauteux, F.; Baumann, E.; Delaney, C.E.; Ly, D.; Star, A.T.; et al. Differential Expression of Receptors Mediating Receptor-Mediated Transcytosis (RMT) in Brain Microvessels, Brain Parenchyma and Peripheral Tissues of the Mouse and the Human. *Fluids and Barriers of the CNS* **2020**, *17*, doi:10.1186/s12987-020-00209-0.
33. Crielaard, B.J.; Lammers, T.; Rivella, S. Targeting Iron Metabolism in Drug Discovery and Delivery. *Nature Reviews Drug Discovery* **2017**, doi:10.1038/nrd.2016.248.
34. Drakesmith, H.; Nemeth, E.; Ganz, T. Ironing out Ferroportin. *Cell Metabolism* **2015**, *22*, 777–787, doi:10.1016/j.cmet.2015.09.006.
35. Gulec, S.; Anderson, G.J.; Collins, J.F. Mechanistic and Regulatory Aspects of Intestinal Iron Absorption. *AJP: Gastrointestinal and Liver Physiology* **2014**, *307*, G397–G409, doi:10.1152/ajpgi.00348.2013.
36. Belaidi, A.A.; Bush, A.I. Iron Neurochemistry in Alzheimer's Disease and Parkinson's Disease: Targets for Therapeutics. *Journal of Neurochemistry* **2016**, *139*, 179–197, doi:10.1111/jnc.13425.
37. Silva, B.; Faustino, P. An Overview of Molecular Basis of Iron Metabolism Regulation and the Associated Pathologies. *Biochimica et biophysica acta* **2015**, *1852*, 1347–1359, doi:10.1016/j.bbadis.2015.03.011.
38. Helgudottir, S.S. Expressional Prerequisites for Targeted Drug Delivery to the Pathological Brain. **2021**, doi:10.54337/AAU424058297.
39. Rouault, T.A. The Role of Iron Regulatory Proteins in Mammalian Iron Homeostasis and Disease. *Nature chemical biology* **2006**, *2*, 406–414, doi:10.1038/NCHEMBIO807.
40. Morgan, E.H.; Moos, T. Mechanism and Developmental Changes in Iron Transport across the Blood-Brain Barrier. *Developmental neuroscience* **2002**, *24*, 106–113, doi:10.1159/000065699.
41. Moos, T.; Oates, P.S.; Morgan, E.H. Expression of the Neuronal Transferrin Receptor Is Age Dependent and Susceptible to Iron Deficiency. *Journal of Comparative Neurology* **1998**, *398*, 420–430, doi:10.1002/(SICI)1096-9861(19980831)398:3<420::AID-CNE8>3.0.CO;2-1.
42. Taylor, E.M.; Crowe, A.; Morgan, E.H. Transferrin and Iron Uptake by the Brain: Effects of Altered Iron Status. *Journal of neurochemistry* **1991**, *57*, 1584–1592, doi:10.1111/J.1471-4159.1991.TB06355.X.
43. Moos, T.; Morgan, E.H. Restricted Transport of Anti-Transferrin Receptor Antibody (OX26) through the Blood-Brain Barrier in the Rat. *Journal of Neurochemistry* **2001**, *79*, 119–129, doi:10.1046/j.1471-4159.2001.00541.x.
44. Burkhart, A.; Skjørringe, T.; Johnsen, K.B.; Siupka, P.; Thomsen, L.B.; Nielsen, M.S.; Thomsen, L.L.; Moos, T. Expression of Iron-Related Proteins at the Neurovascular Unit Supports Reduction and Reoxidation of Iron for Transport Through the Blood-Brain Barrier. *Molecular Neurobiology* **2016**, *53*, 7237–7253, doi:10.1007/s12035-015-9582-7.
45. Gelder, W. Van; Huijskes-Heins, M.I.E.; Dijk, J.P. Van; Cleton-Soeteman, M.I.; Eijk, H.G. Van Quantification of Different Transferrin Receptor Pools in Primary Cultures of Porcine Blood-Brain Barrier Endothelial Cells. *Journal of Neurochemistry* **1995**, *64*, 2708–2715, doi:10.1046/J.1471-4159.1995.64062708.X.
46. Daneman, R.; Zhou, L.; Agalliu, D.; Cahoy, J.D.; Kaushal, A.; Barres, B.A. The Mouse Blood-Brain Barrier Transcriptome: A New Resource for Understanding the Development and Function of Brain Endothelial Cells. *PloS one* **2010**, *5*, e13741, doi:10.1371/journal.pone.0013741.
47. Simpson, I.A.; Carruthers, A.; Vannucci, S.J. Supply and Demand in Cerebral Energy Metabolism: The Role of Nutrient Transporters. *Journal of cerebral blood flow and metabolism : official journal of the International Society of Cerebral Blood Flow and Metabolism* **2007**, *27*, 1766–1791, doi:10.1038/sj.jcbfm.9600521.
48. Simpson, I.A.; Vannucci, S.J.; DeJoseph, M.R.; Hawkins, R.A. Glucose Transporter Asymmetries in the Bovine Blood-Brain Barrier. *Journal of Biological Chemistry* **2001**, *276*, 12725–12729, doi:10.1074/jbc.M010897200.
49. Winkler, E.A.; Nishida, Y.; Sagare, A.P.; Rege, S. V.; Bell, R.D.; Perlmutter, D.; Sengillo, J.D.; Hillman, S.; Kong, P.; Nelson, A.R.; et al. GLUT1 Reductions Exacerbate Alzheimer's Disease Vasculo-Neuronal Dysfunction and Degeneration. *Nature Neuroscience* **2015**, *18*, 521–530, doi:10.1038/nn.3966.

 doi:10.20944/preprints202404.1939.v1




50. Guo, X.; Geng, M.; Du, G. Glucose Transporter 1, Distribution in the Brain and in Neural Disorders: Its Relationship with Transport of Neuroactive Drugs through the Blood-Brain Barrier. *Biochemical genetics* **2005**, *43*, 175–187, doi:10.1007/s10528-005-1510-5.
51. Leclerc, M.; Tremblay, C.; Bourassa, P.; Schneider, J.A.; Bennett, D.A.; Calon, F. Lower GLUT1 and Unchanged MCT1 in Alzheimer's Disease Cerebrovasculature. *Journal of cerebral blood flow and metabolism : official journal of the International Society of Cerebral Blood Flow and Metabolism* **2024**, doi:10.1177/0271678X241237484.
52. Chew, K.S.; Wells, R.C.; Moshkforoush, A.; Chan, D.; Lechtenberg, K.J.; Tran, H.L.; Chow, J.; Kim, D.J.; Robles-Colmenares, Y.; Srivastava, D.B.; et al. CD98hc Is a Target for Brain Delivery of Biotherapeutics. *Nature Communications* **2023**, *14*, doi:10.1038/s41467-023-40681-4.
53. Uchida, Y.; Ohtsuki, S.; Katsukura, Y.; Ikeda, C.; Suzuki, T.; Kamiie, J.; Terasaki, T. Quantitative Targeted Absolute Proteomics of Human Blood-Brain Barrier Transporters and Receptors. *Journal of Neurochemistry* **2011**, *117*, 333–345, doi:10.1111/j.1471-4159.2011.07208.x.